

CaDM: Codec-aware Diffusion Modeling for Neural-enhanced Video Streaming

Qihua Zhou, Ruibin Li, Song Guo, Peiran Dong, Yi Liu, Jingcai Guo, Zhenda Xu
Department of Computing, The Hong Kong Polytechnic University

{qi-hua.zhou, ruibin.li, peiran.dong, joeylau.liu, jackal.xu}@connect.polyu.hk
{song.guo, jc-jingcai.guo}@polyu.edu.hk

Abstract

Recent years have witnessed the dramatic growth of Internet video traffic, where the video bitstreams are often compressed and delivered in low quality to fit the streamer’s uplink bandwidth. To alleviate the quality degradation, it comes the rise of Neural-enhanced Video Streaming (NVS), which shows great prospects for recovering low-quality videos by mostly deploying neural super-resolution (SR) on the media server. Despite its benefit, we reveal that current mainstream works with SR enhancement have not achieved the desired rate-distortion trade-off between bitrate saving and quality restoration, due to: (1) overemphasizing the enhancement on the decoder side while omitting the co-design of encoder, (2) limited generative capacity to recover high-fidelity perceptual details, and (3) optimizing the compression-and-restoration pipeline from the resolution perspective solely, without considering color bit-depth. Aiming at overcoming these limitations, we are the first to conduct an encoder-decoder (i.e., codec) synergy by leveraging the inherent visual-generative property of diffusion models. Specifically, we present the Codec-aware Diffusion Modeling (CaDM), a novel NVS paradigm to significantly reduce streaming delivery bitrates while holding pretty higher restoration capacity over existing methods. First, CaDM improves the encoder’s compression efficiency by simultaneously reducing resolution and color bit-depth of video frames. Second, CaDM empowers the decoder with high-quality enhancement by making the denoising diffusion restoration aware of encoder’s resolution-color conditions. Evaluation on public cloud services with OpenMMLab benchmarks shows that CaDM effectively saves up to 5.12 – 21.44× bitrates based on common video standards and achieves much better recovery quality (e.g., FID of 0.61) over state-of-the-art neural-enhancing methods.

1. Introduction

The video traffic has experienced tremendous growth with the emergence of Internet streaming services (e.g.,

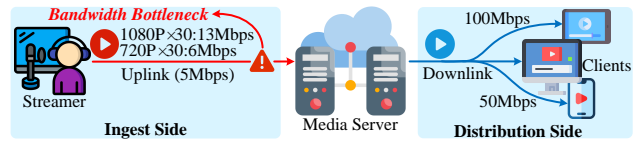


Figure 1. Overview of a common video streaming infrastructure [70, 26, 68].

Zoom meeting [80], YouTube live [73] and Netflix [44]) over the last decade. As shown in Figure 1, today’s video streaming infrastructure usually consists of two sides: (1) the ingest side where the streamer uploads video bitstreams to the media server through the streamer’s uplink [67, 43, 29, 11], and (2) the distribution side where the server broadcasts the prepared videos to clients through the server’s downlink [34, 48, 24, 39]. The ingest side often requires low-latency streaming protocols for video delivery [54, 23, 52, 28] and the distribution side involves the deployment of adaptive bitrate (ABR) algorithms [48, 47, 63, 65] to match client’s Quality of Experience (QoE) [75, 69, 1, 72]. Consistent with recent mainstream works [36, 70, 15], this paper focuses on the video streaming performance on the ingest side, i.e., involving the uplink from the streamer to the server.

Unfortunately, a practical issue is that the streamer’s uplink bandwidth is usually far lower than the server’s downstream bandwidth [75, 45, 10], making the ingest side become the performance bottleneck for continuously delivering high-definition videos [70, 36, 15]. To fit the limited uplink bandwidth, a natural methodology is to compress the video bitstreams in low quality for realizing communication-efficient delivery, e.g., from 1080p/720p to 360p. The frame compression usually involves two key perspectives: (1) the downscaling of spatial resolution [27, 31, 79, 25] and (2) the reduction of color bit-depth to represent a pixel [37, 35, 41, 76]. Obviously, compression from either perspective will deprive the server from obtaining high-quality videos and finally hampers the perceptual experience of downstream distribution services, especially when video quality often significantly impacts

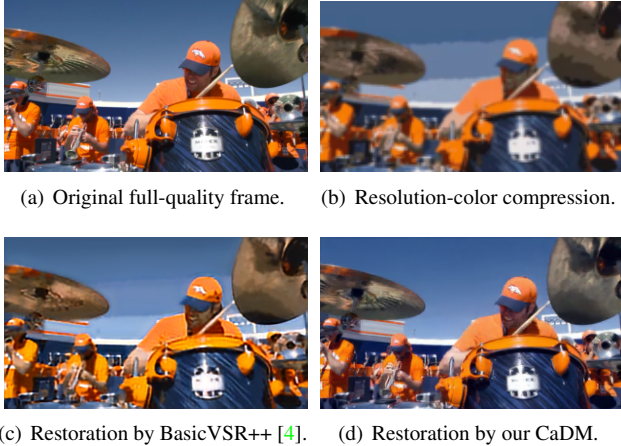


Figure 2. Visualization of neural-enhanced video streaming in different stages: (a) the original full-quality frame, (b) encoder’s resolution-color compression, (c) decoder’s restoration by SOTA BasicVSR++ [4], and (d) decoder’s restoration by our CaDM that achieving pretty higher enhancement quality over BasicVSR++.

user’s engagement in video streaming [12, 14, 30, 78, 58]. To alleviate the performance bottleneck on the ingest side in current video streaming infrastructure, it comes the rise of *Neural-enhance Video Streaming* (NVS) paradigm [70, 36, 15, 26, 68, 10], where a majority of works aim to restore the compressed video quality by deploying a neural super-resolution (SR) model on the media server [70, 75, 45, 26, 68, 62]. The restored videos should hold sufficient visual quality as the original version, so as to guarantee the service experience of downstream video distribution. Consequently, the core objective of NVS is to reduce the delivery bitrates while restricting the quality distortion of restored videos in an acceptable range.

However, our preliminary experiments verified that current mainstream works with SR enhancement have not achieved a desired *rate-distortion* trade-off between bitrate saving and quality restoration. As illustrated in Figure. 2, we visualize the original, compressed and restored frames in the NVS pipeline. It is clear that even adopting state-of-the-art (SOTA) BasicVSR++ method [4] cannot guarantee a desired quality restoration when the frame is compressed with low spatial resolution and color bit-depth. We reveal that existing SR-based NVS methods fall short of restoring low-quality frames due to: (1) overemphasizing the enhancement on the decoder side while omitting the co-design of encoder, (2) inherent limited restoration capacity to generate high-fidelity perceptual details, and (3) optimizing the compression-and-enhancement pipeline from the resolution perspective solely, without considering color bit-depth.

These limitations motivate us to improve the encoder-decoder (*i.e.*, codec) synergy and design a new NVS paradigm to significantly reduce delivery bitrates while pro-

viding a much higher restoration capacity over existing methods. To achieve this target, we present the *Codec-aware Diffusion Modeling* (CaDM), which efficiently restores the low-quality videos by leveraging the visual-generative property of diffusion models. First, CaDM improves the encoder’s compression efficiency by simultaneously reducing resolution and color bit-depth of video frames (§3.2). Second, CaDM provides the decoder with powerful quality enhancement by making the denoising diffusion restoration aware of encoder’s resolution-color conditions (§3.3). Extensive experiments on public cloud services with OpenMMLab benchmarks show that CaDM significantly saves delivery bitrates by 5.12 – 21.44× reduction on top of common video standards (*e.g.*, H.264/AVC [17], H.265/HEVC [18] and H.266/VVC [19]) and achieves higher recovery quality over state-of-the-art methods.

In summary, our key contributions are as follows.

- **Novel NVS paradigm.** To the best of our knowledge, CaDM is the first work to essentially solve the key bottleneck on the ingest side of video streaming infrastructure. It conducts an encoder-decoder synergy (§3.1) to significantly improve the *rate-distortion* trade-off against current NVS paradigm.
- **High compression ratio.** CaDM effectively fits the streamer’s uplink capacity and reduces the video delivery bitrates by an order of magnitude. It improves the encoder’s compression efficiency by simultaneously downscaling the spatial resolution (§3.2.1) and reducing the color bit-depth (§3.2.2). Thus, CaDM can serve as a general and auxiliary compression-enhancement module to further improve existing video standards.
- **State-of-the-art restoration performance.** CaDM leverages the visual-generative property of diffusion models to improve decoder’s enhancement capacity (§3.3), achieving state-of-the-art restoration performance in different quality assessment metrics (§4.2).

2. Related Work

2.1. Neural-enhanced Video Streaming

Recall the video streaming infrastructure in Figure. 1, alleviating the uplink bottleneck is a crucial issue on the ingest side, which promotes the rise of *Neural-enhanced Video Streaming* (NVS) [70, 36, 15, 26, 68, 10] paradigm. To improve the video delivery performance, NVS involves the collaboration between streamer and server. First, the streamer downscales the original high-resolution video frames into the low-resolution version, then encodes the frames into video bitstreams for network transmission. The media server decodes the bitstreams as a series of frames and fed them into a neural super-resolution (SR) model for quality enhancement [70, 75, 45, 26, 68]. The final

restored video holds comparable visual experience as the original version, thus can be applied to the content distribution in different downstream tasks. Recently, optimizing the NVS pipeline has become a hot topic, including improving video encoding efficiency [15, 10], reducing steaming latency [69], designing adaptive bit-rate delivery [10] and optimizing SR enhancement [66, 74, 45]. Overall, the core objective of an efficient NVS paradigm is to improve the *rate-distortion* trade-off for video delivery, *i.e.*, reducing streaming bitrates while restricting quality drop after restoration.

2.2. Neural-enhancing Models

Restoring the compressed videos with high-fidelity visual details is a fundamental component of NVS paradigm. Current mainstream NVS frameworks often employ a neural super-resolution (SR) model for quality enhancement. Modern SR techniques mainly exploit the power of deep neural networks, aiming at transferring the low-resolution image to high-resolution version, *e.g.*, EDSR [31], EUSR [6] and FRSR [55]. As the video consists of a series of frames, the SR model can also be applied to enhance video quality, *e.g.*, IconVSR [3], RealBasicVSR [5] and BasicVSR++ [4]. Some modern video SR models also leverage the generative networks to compensate spatial-temporal coherence across frames, *e.g.*, TecoGAN [8], PULSE [42] and Real-ESRGAN [59]. Recently, the diffusion probabilistic models (*e.g.*, DDPM [21], DDIM [56] and LDM [49]) have achieved impressive performance in diverse generative tasks, including inpainting [40], colorization [57] and image synthesis [50]. Inspired by the latest research progress of neural-enhancing models, we intend to conduct the encoder-decoder (*i.e.*, codec) synergy by leveraging the visual-generative capacity of diffusion models. We present the *Codec-aware Diffusion Modeling* (CaDM, §3), a novel NVS paradigm to significantly improve the *rate-distortion* trade-off over SOTA methods.

3. Codec-aware Diffusion Modeling

3.1. Problem Formulation and Objective

Traditional video streaming. As a video consists of a series of frames \mathbf{x} , we use x_i to denote an original raw high-quality frame with index i , where $x_i \in \mathbf{x}$ and i identifies the sequence order for video encoding. After encoding all the frames as a high-quality video, the video bitstreams will be delivered through the network to the ingest server. The server receives the bitstreams and decodes it for downstream tasks. We can adopt common video standards (*e.g.*, H.264/AVC [17], H.265/HEVC [18] and H.266/VVC [19]) to handle the entire encoder-decoder procedure and formulate the traditional video streaming pipeline $f(\cdot)$ as:

$$f(\mathbf{x}) = \text{Decode}(\text{Encode}(\mathbf{x})). \quad (1)$$

Neural-enhanced video streaming. Recent NVS researches [70, 15, 26, 68, 10] have shown that directly encoding the video from raw frames and delivering the high-quality video through network is impractical due to streamer’s limited uplink bandwidth. Conducting frame compression before video encoding is necessary to fit the bandwidth restriction, where downscaling the frame resolution with a constant scaling factor (*e.g.*, from 720p to 360p with a $2\times$ factor) is the mainstream methodology [70, 75, 45, 26, 68, 44]. As a result, practical NVS frameworks usually encode a low-resolution video based on the downscaled frames, deliver the video bitstreams through the network, and decode the bitstreams to a series of low-quality frames for subsequent processing. Since the frame quality is degraded, a pre-trained neural super-resolution (SR) model is adopted by the decoder to recover the visual quality. The SR-enhanced decoder transfers the low-resolution frames back to the high-resolution version, *e.g.*, upscaling the 360p frames to the 720p ones [70, 75, 45]. Thus, a typical NVS pipeline can be described as:

$$f(\mathbf{x}) = \text{Decode}(\text{Encode}(\mathbf{x}; s); \text{SR}), \quad (2)$$

where s is the scaling factor used in resolution downscaling and the neural SR model.

Our CaDM paradigm. Different from existing work, we reveal that the color bit-depth, *i.e.*, the number of bits to represent a unique pixel in visual, has not been well exploited to further reduce the frame size. Figure. 3 illustrates the pipeline of our CaDM’s paradigm. By conducting the frame compression from bit-depth and resolution perspectives simultaneously, the encoder can achieve a much higher compression ratio over the existing NVS methods. However, as more visual information has been compressed, we need a more powerful enhancement module to restore the perceptual details. As verified by our preliminary experiments in Figure. 2, conventional SR models used by current NVS cannot achieve a desired restoration performance when using high compression ratios. This motivates us to re-design the neural enhancement by leveraging the visual-generative property of diffusion models. We design the *Codec-aware Diffusion Modeling* (CaDM), a novel NVS paradigm, to achieve this target. Together with the resolution scaling factor s , color bit-depth n , and diffusion model parameters θ , the entire pipeline of our CaDM can be formulated as:

$$f(\mathbf{x}) = \text{Decode}(\text{Encode}(\mathbf{x}; s, n); \theta). \quad (3)$$

Objective. By embedding the variables of s and n into diffusion conditions (§3.3.1), our objective is to optimize CaDM by training on public video datasets (§3.3.2) to *minimize the gap between restored video frames $f(\mathbf{x})$ and the original ones \mathbf{x}* . We will discuss how CaDM handles the encoder-decoder synergy in the following sections.

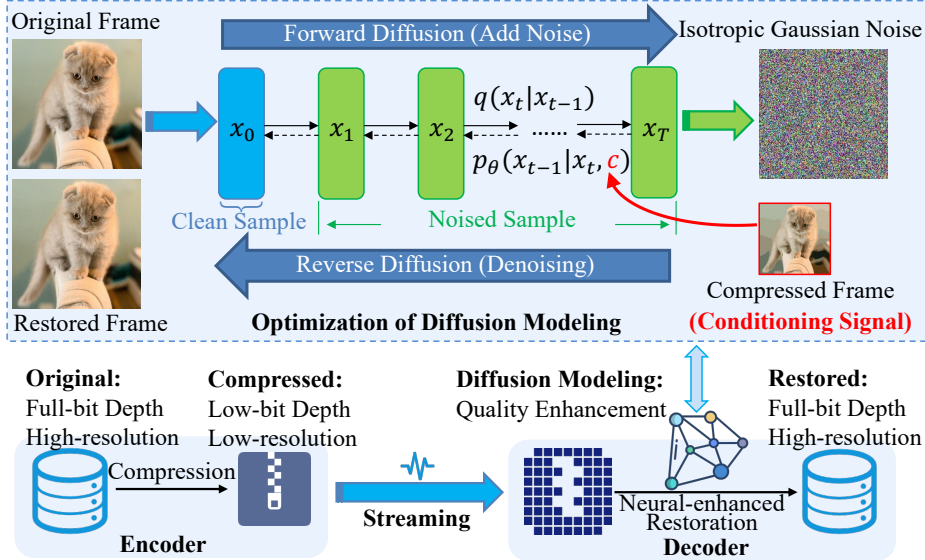


Figure 3. Pipeline of our CaDM paradigm, which restores low-quality videos from both frame resolution and color bit-depth.

3.2. Encoder with Resolution-color Compression

The role of CaDM’s encoder is to reduce the video size with a much higher compression ratio over existing NVS methods, so as to save the delivery bitrates. Note that an extreme compression will lead to a significant degradation on frame visual quality, which may exceed the restoration capacity of the neural-enhancement model on the decoder. We cannot introduce an arbitrary compression mechanism, but need to conduct compression based on the decoder’s restoration property. Thus, we handle the compression from two aspects: (1) downscaling the frame resolution in §3.2.1 and (2) reducing the pixel color bit-depth in §3.2.2.

3.2.1 Patch-wise Resolution Downscaling

The first compression perspective is to downscale the frame resolution, *i.e.*, shrinking the spatial size under the control of a scaling factor s . As the number of pixels within the frame is reduced in both width and height dimensions, resolution downscaling can provide a $s^2 \times$ frame size reduction compared with the original frame. Although fewer pixels are used to represent a frame, its basic visual features should be preserved, otherwise, the visual quality degradation will exceed the decoder’s recovery capacity. This property requires the scaling algorithm to retain the most representative pixels by analyzing the numerical distribution in each frame patch (*i.e.*, the macroblock, a non-overlapping square block with $s \times s$ pixels in visual). As a preliminary concept to video codec, patch can serve as the basic processing units to explore intra- and inter-frame correlation [70, 10, 26, 68, 69]. In default, we suggest using 4×4 patch size, which is a sufficient fine-grained granularity to retain visual features after downscaling. Therefore, as for

each pixel, we can figure out a patch where this pixel locates in the center. Specifically, considering the pixels on the frame border, we adopt zero-padding to the border with $\lceil \frac{s}{2} \rceil$ pixels in width and height, so as to guarantee complete patches. Given a scaling factor s , we can divide the frame into a series of $s \times s$ patches. Based on the patch division, we introduce a *Gaussian Blur* to the frame and smooth the features involving a junction of patches. Inside each patch, we calculate the weighted average of all the pixels inside and shrink the patch by this average. Thus, the entire frame is downscaled by $s \times$ in both width and height dimensions.

3.2.2 Color Bit-depth Quantization

The second compression perspective is to reduce the color bit-depth, *i.e.*, the number of bits to identify a unique pixel. As to common video standards, the source frames are usually organized with 8-bit color space with RGB channels. Therefore, each pixel within a frame is represented in 24 bits, which is similar to the color space of PNG and JPEG formats [37, 35]. Meanwhile, the pixel vectors along the RBG channel hold similar distributions when they describe close colors in visual. This motivates us to revisit the *Vector Quantization* [16, 32, 9, 38] technique and reduce the number of different colors represented by the pixels. For example, if we quantize the color space into 4 bits with 2^4 different colors, the frame size can be compressed into $4/24$ as the original frame with full-color bit-depth. The key here is to find a proper vector quantization scheme to transfer the full bit-depth pixels into low bit-depth ones. Specifically, we use the K-means clustering to handle the quantization procedure, which contains the following two steps. Although recent video standards rarely use vector quantization, we believe introduce this technique can further im-

prove encoder’s compression ratio.

Step #1: Codebook generation. This step aims at generating the quantization codebook that maps all pixels from full color bit-depth to low bit-depth, *e.g.*, from original 24-bit color space to 4-bit version. This requires us to group all the pixels within the frames into several clusters and represent all the pixels belonging to the same cluster by its centroid, so as to reduce the information entropy (reflected by number of bits) to identify each unique pixel. Here, the number of clusters is called the quantization level, which directly impacts the representation precision of the pixel color space. If we adopt n -bit to generate the quantization codebook, all the pixels will be grouped into 2^n clusters. In our CaDM, n is set in range of [4, 8] to greatly reduce frame size over the original 24-bit color space. Given n -bit budget to represent the color space, we choose the K-means clustering to generate the quantization codebook. Note that we need to restrict the computational overhead of calculating K-means clustering model because it iteratively calculates the neighbourhood distance for each pixel. Although we have downscaled the resolution before color quantization, the pixel number of low-resolution frame is still in order of magnitude of $10^5 - 10^6$. In this case, directly adopting K-means on the entire frame pix is computational unacceptable. To address this challenge, we uniformly sample a subset of pixels (usually in order of magnitude of 10^3) from the frame and obtain K-means clustering model based on these samples. The K-means model describes how to map all the pixels into 2^n clusters and figures out the all cluster centriods. Each centriod is assigned with a unique index, ranging from 0 to $2^n - 1$. Therefore, the gist of our quantization codebook is to map each pixel to its corresponding cluster centriod, which can be represented by n bits.

Step #2: Pixel quantization. Based on the first step of generating quantization codebook, the second step is to replace each pixel by its cluster centriod. The original pixel matrix describing a frame can be transferred as the centroid matrix with the same shape, where each element corresponds to the pixel’s centriod. As a result, the original full bit-depth pixels are quantized into n bit-depth version. The frame size is compressed to $\frac{n}{24}$ of the raw frame in 24-bit color space. In realistic deployment, the codebook can be obtained and sent to the ingest server in advance. Therefore, the communication cost for transmitting codebook can be omitted.

Summary. Theoretically, given the scaling factor s and color bit-depth n , we can figure out the entire compression ratio over traditional 24-bit full-resolution frames as $\frac{24s^2}{n}$. Therefore, the encoder contributes to the resolution-color compression and reduces the bitrates of video streaming.

3.3. Decoder with Denoising Diffusion Restoration

On the streamer side, our CaDM’s encoder aims at providing a great compression ratio to reduce video delivery

bitrates. Meanwhile, we deploy CaDM’s decoder on the ingest server to recover the video bitstreams and enhance the visual quality by leveraging the visual-generative property of diffusion models. As a kind of generative model, we optimize the decoder based on probabilistic theory. The gist of our decoder is to recover the low-quality video bitstreams through a series of denoising steps. Inside each step, we try to minimize the gap between predicted noise and the true noise, which is handled by a pre-trained diffusion model. The diffusion model is established with two key concepts: (1) distortion-aware conditioning (§3.3.1) that guides model to generate high-fidelity visual details after a series of denoising steps, and (2) training the diffusion model (§3.3.2) to correctly predict the noise that should be removed to restore the frame in each step.

3.3.1 Distortion-aware Conditioning

Similar to latest conditioned generative models, we need a conditioning signal c to guide the decoder: *generating what kind of frames can minimize the fidelity gap from the original frames?* Here, the decoder should be aware of the frame distortion caused by the encoder. Therefore, we need to embed the frame distortion into conditioning signal so that the model can correctly learn the conditional probability to generate high-fidelity frames like the realistic ones. As low-quality videos are received by the ingest server, the decoder can capture all the compressed frames and upscale them to original resolution by using the fast bilinear interpolation. Following the mainstream mechanism to handle the conditioning [50], the decoder initializes a Gaussian noise as the generative seed and concatenates the upscaled frames with it along the channel dimension. The diffusion model takes the concatenation result to generate high-quality frames.

3.3.2 Model Training and Frame Restoration

Based on the discussion of embedding conditioning signals, the next step is to train the diffusion model for frame restoration. The training procedure contains two stages: (1) forward diffusion and (2) reverse diffusion. Here, we present key formulations of these two stages.

Forward diffusion. Given the original data distribution of the frames that $\mathbf{x} \sim q(\mathbf{x})$, the forward stage aims at gradually degrading the frame quality by inserting a small amount of Gaussian noise $\epsilon \sim \mathcal{N}(0, \mathbf{I})$ into the frame through T steps. Based on the original frame \mathbf{x}_0 at the beginning, the core formulation of degraded frame \mathbf{x}_t in the t -th step ($t \in [1, T]$) can be described as:

$$\mathbf{x}_t = \sqrt{\alpha_t}\mathbf{x}_{t-1} + \sqrt{1 - \alpha_t}\epsilon_{t-1}, \quad (4)$$

where the hyper-parameter $0 < \alpha_t < 1$ controls the variance of the noise inserted in each step. Therefore, the frame

\mathbf{x}_T will entirely lose the visual features after T steps. When $T \rightarrow +\infty$, \mathbf{x}_T is equivalent to an isotropic Gaussian distribution. Accumulating all the T steps, we can obtain the final degraded frame \mathbf{x}_T as:

$$\mathbf{x}_T = \sqrt{\bar{\alpha}_T} \mathbf{x}_0 + \sqrt{1 - \bar{\alpha}_T} \boldsymbol{\epsilon}, \quad (5)$$

where $\bar{\alpha}_T = \prod_{t=1}^T \alpha_t$. Thus, we can formulate the final status of the forward diffusion as:

$$q(\mathbf{x}_T | \mathbf{x}_0) = \mathcal{N}(\mathbf{x}_T; \sqrt{\bar{\alpha}_T} \mathbf{x}_0, (1 - \bar{\alpha}_T) \mathbf{I}). \quad (6)$$

Briefly, the forward diffusion will gradually insert Gaussian noise into all the frames and finally make them equivalent to an isotropic Gaussian distribution.

Reverse diffusion. As to the frame restoration, we need to reverse the forward process of the diffusion model. This procedure is the major learning objective of our CaDM, which can be formulated as:

$$q(\mathbf{x}_{t-1} | \mathbf{x}_t, \mathbf{x}_0) = q(\mathbf{x}_t | \mathbf{x}_{t-1}, \mathbf{x}_0) \frac{q(\mathbf{x}_{t-1} | \mathbf{x}_0)}{q(\mathbf{x}_t | \mathbf{x}_0)}. \quad (7)$$

Therefore, we can train the diffusion model θ to learn this probability by minimizing the gap between the predicted noise $\boldsymbol{\epsilon}_\theta$ and true noise $\boldsymbol{\epsilon}_t$ added in the t -th step during forward stage. Following this principle, we can formulate the corresponding loss function \mathcal{L} as:

$$\begin{aligned} \mathcal{L} &= \mathbb{E}_{t \sim [1, T], \mathbf{x}_0, \boldsymbol{\epsilon}_t} \left[\|\boldsymbol{\epsilon}_t - \boldsymbol{\epsilon}_\theta(\mathbf{x}_t, t, c)\|^2 \right] \\ &= \sum_{t=1}^T \mathbb{E}_{\mathbf{x}_0, \boldsymbol{\epsilon}_t} \left[\|\boldsymbol{\epsilon}_t - \boldsymbol{\epsilon}_\theta(\sqrt{\bar{\alpha}_t} \mathbf{x}_0 + \sqrt{1 - \bar{\alpha}_t} \boldsymbol{\epsilon}_t, t, c)\|^2 \right], \quad (8) \end{aligned}$$

where t is the denoising level reflected by the step index, \mathbf{x}_t is the restored sample in step t , and c is the distortion-aware conditions of low-quality video frames. By feeding these variables into the diffusion model θ , we can optimize CaDM to hold sufficient restoration capacity to generate high-fidelity videos from the compressed bitstreams. In summary, the training procedure to generate the diffusion model and inference procedure to restore frame quality are summarized in Algorithm 1 and Algorithm 2, respectively.

Summary. The diffusion model inside the decoder serves as an enhancement module to recover the video quality by perceiving encoder’s resolution-color compression. We have restricted CaDM’s computational complexity to fit the video streaming environment. In the video ingest scenarios [70], CaDM’s enhancement procedure is deployed on the media server rather than the user client. The commodity hardware (e.g., GPUs and TPUs) on media server is powerful enough to conduct the enhancement operations. For example, enhancing a 10-second video only takes 830ms when using TPU-v3-8 chips and LDM [49] sampling, i.e., lower than 8.3% additional time cost is incurred. Therefore, CaDM is efficient to handle common video streaming.

Algorithm 1 Training diffusion model θ until convergence

Input: original frames \mathbf{x} , scaling factor s , bit-depth n .

Output: converged model θ .

- 1: $\hat{\mathbf{x}} = \text{Encode}(\mathbf{x}; s, n)$; ▷ Get the compressed frames.
 - 2: **repeat**
 - 3: $c \leftarrow \text{Upscale}(\hat{\mathbf{x}})$; ▷ Fast bilinear interpolation.
 - 4: $t \sim \text{Uniform}(1, \dots, T)$; ▷ Step index sampling.
 - 5: $\boldsymbol{\epsilon} \sim \mathcal{N}(\mathbf{0}, \mathbf{I})$; ▷ Gaussian noise.
 - 6: Take gradient descent step on:
 - 7: $\nabla_{\theta} \|\boldsymbol{\epsilon}_t - \boldsymbol{\epsilon}_\theta(\sqrt{\bar{\alpha}_t} \mathbf{x} + \sqrt{1 - \bar{\alpha}_t} \boldsymbol{\epsilon}_t, t, c)\|^2$;
 - 8: **until** θ is converged; ▷ End with a converged model.
-

Algorithm 2 Inference in T steps for frame restoration

Input: compressed frames $\hat{\mathbf{x}}$, pre-trained model θ .

Output: restored frames $\tilde{\mathbf{x}}$.

- 1: $\mathbf{x}_T \sim \mathcal{N}(\mathbf{0}, \mathbf{I})$;
 - 2: $c \leftarrow \text{Upscale}(\hat{\mathbf{x}})$; ▷ Fast bilinear interpolation.
 - 3: **for** $t \in T, \dots, 1$ **do**
 - 4: $\mathbf{z} \sim \mathcal{N}(\mathbf{0}, \mathbf{I})$; ▷ Gaussian seed.
 - 5: $\Delta \mathbf{x}_0 \leftarrow \frac{\sqrt{\bar{\alpha}_{t-1}} \mathbf{x}_t - \sqrt{1 - \bar{\alpha}_t} \boldsymbol{\epsilon}_\theta(\mathbf{x}_t, t, c)}{\sqrt{\bar{\alpha}_t}}$;
 - 6: $\Delta \mathbf{x}_t \leftarrow \sqrt{1 - \bar{\alpha}_{t-1} - \sigma_t^2} \boldsymbol{\epsilon}_\theta(\mathbf{x}_t, t, c)$;
 - 7: $\sigma_t^2 \leftarrow \frac{1 - \bar{\alpha}_{t-1} - \alpha_t}{1 - \bar{\alpha}_t}$;
 - 8: $\mathbf{x}_{t-1} \leftarrow \Delta \mathbf{x}_0 + \Delta \mathbf{x}_t + \sigma_t \mathbf{z}$;
 - 9: **end for** ▷ End loop with \mathbf{x}_0 .
 - 10: $\tilde{\mathbf{x}} \leftarrow \mathbf{x}_{t-1}$;
 - 11: **Return** $\tilde{\mathbf{x}}$;
-

4. Evaluation

4.1. Experimental Setups

Benchmarks and Baselines. To match the runtime environment of realistic NVS pipelines, we evaluate CaDM with OpenMMLab [46] benchmarks and handle the video streaming by common video standards, including H.264/AVC [17], H.265/HEVC [18] and H.266/VVC [19]. We consider seven typical SR baselines with diverse model architectures, including SOTA BasicVSR++ [4], RealBasicVSR [5], IconVSR [3], MSRResNet [77], ESRGAN [60], EDSR [31], and SRCNN [13]. Following previous works [4, 3, 5], we use Vimeo-90K [64] as the training set, and use UDM10 [71] and Vid4 [33] as test sets. We conduct resolution-color compression (§3.2) to obtain low-quality videos, which are used for streaming delivery and video restoration. To guarantee comparison fairness, we re-train the seven baselines under the same application scenario as the proposed CaDM method, i.e., the low-quality and original videos serve as the input and ground-truth, respectively.

Performance measurement. As to encoder’s compression efficiency, we inspect how CaDM reduces the video delivery bitrates (Kbps), which is directly proportional to the

Model	UDM10 [71]				Vid4 [33]			
	FID ↓	IS ↑	SSIM ↑	PSNR ↑	FID ↓	IS ↑	SSIM ↑	PSNR ↑
BasicVSR++ [4]	3.91	3.07±0.49	0.76	31.91	8.28	1.21±0.06	0.42	26.12
RealBasicVSR [5]	3.43	3.07±0.72	0.78	32.29	5.78	1.19±0.05	0.75	28.34
IconVSR [3]	2.89	3.10±0.40	0.81	32.53	5.32	1.20±0.06	0.74	28.39
MSRResNet [77]	4.17	3.04±0.42	0.77	31.92	10.04	1.20±0.07	0.69	28.03
ESRGAN [60]	4.73	2.99±0.67	0.75	31.53	18.48	1.14±0.04	0.58	27.43
EDSR [31]	3.73	2.92±0.45	0.75	31.56	12.29	1.10±0.03	0.62	27.66
SRCNN [13]	6.84	2.89±0.56	0.70	31.08	22.34	1.10±0.04	0.58	27.40
CaDM (Ours)	0.61	3.12±0.22	0.86	32.32	1.97	1.23±0.05	0.82	29.19

Table 1. Comparison with SOTA neural-enhancing methods, where the red and blue colors indicate the best and the second-best performance, respectively. The videos are compressed with 4× scaling factor and 4-bit color space.

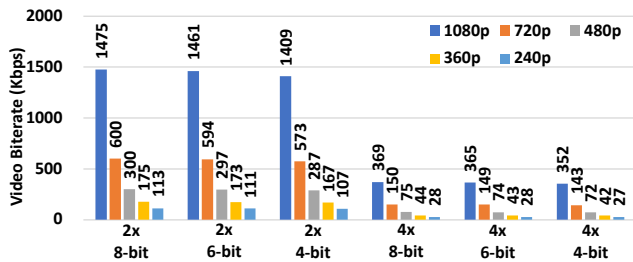


Figure 4. Average video bitrates (Kbps) using different resolution-color settings, where original bitrates of 1080p, 720p, 480p, 360p, and 240p achieved by vanilla video standards are 7552, 3072, 1536, 896 and 576, respectively.

size of streaming traffic. Also, as to decoder’s restoration performance, we calculate the *Fréchet Inception Distance* (FID) [20], *Inception Score* (IS) [51], *Structural Similarity Index Method* (SSIM) [61] and *Peak Signal-to-noise Ratio* (PSNR) [22] between the restored videos and the original ones. FID is the lower the better, while IS, SSIM and PSNR are the opposite. These are modern quality assessment metrics used by latest neural-enhancing works [50, 49, 56, 57, 40]. We deeply inspect CaDM’s *rate-distortion* trade-off between streaming bitrate saving and video quality restoration. Ablation studies of resolution scaling factor, color bit-depth, and built-in bitrate factors are also discussed. Due to the page limit, we present core results here. More detailed training settings, quantified analysis, and visualization are in the supplementary materials.

4.2. End-to-end Performance

Inspection of Bitrate Saving. Saving video bitrates is the first objective of an efficient NVS paradigm. As shown in Figure 4, we inspect the video bitrates (Kbps) achieved by CaDM’s encoder under different resolution-color settings. The resolution scaling factor is from 2× to 4×, which are suitable to downscale common 1080p and 720p videos. Also, original frames are represented in 24-bit color space while CaDM restricts the color bit-depth in [4, 8]. All the videos are encoded as 30 frames per second. It is clear that

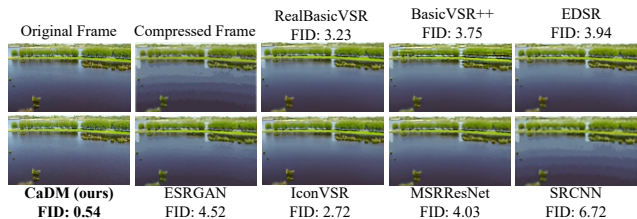


Figure 5. Visualization of restoration performance with different methods. Only CaDM recovers high-fidelity visual details as original one. Please zoom in for best illustration.

CaDM yields much lower video bitrates over vanilla video standard. Under a larger scaling factor and lower color bit-depth (e.g., 4×, 4-bit), CaDM finally achieves up to 21.44× bitrate reduction. This makes CaDM qualified to deliver high-definition 1080p video streaming on the ingest side.

Inspection of Restoration Quality. Apart from bitrate saving, providing high restoration quality is another key objective. As shown in Table 1, CaDM significantly outperforms the seven baselines in terms of FID, IS and SSIM. Here, the FID is a typical metric to compare the distribution between restored frames and the original ones, providing more precise measurement over the earlier IS score. Meanwhile, SSIM is a widely-adopted metric to reflect the perceptual similarity between two frames. The highest scores of FID, IS and SSIM achieved by CaDM guarantee the high restoration quality for human vision, which is visualized by the case in Figure 5. Note that CaDM does not always achieve the highest PSNR because the generative procedure inside CaDM’s diffusion model inserts a series of Gaussian noise to recover the visual details, which enlarges the L2 distance in PSNR. Previous works have verified that PSNR does not necessarily match image perceptual quality [2, 7, 59]. Therefore, FID, IS and SSIM may be more suitable to reflect the restoration performance.

Inspection of Rate-distortion Trade-off. We inspect the *rate-distortion* trade-off between video bitrates and restoration quality, when using CaDM and the seven baselines. The bitrates are adjusted by changing the resolution scal-

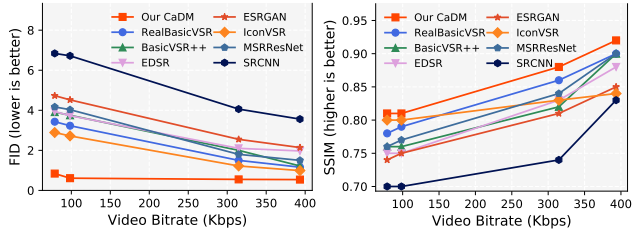


Figure 6. Comparison of the restoration quality to bitrates, where CaDM consistently outperforms existing methods.

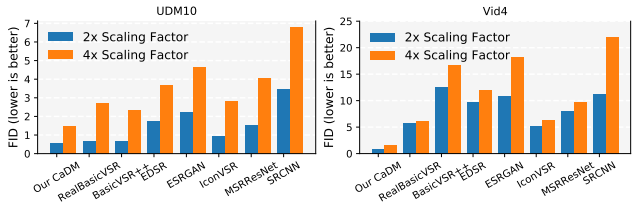


Figure 7. Restoration quality with different resolutions.

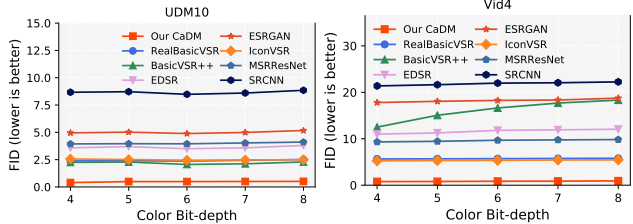


Figure 8. Restoration quality with different color bit-depth.

ing factor and color bit-depth. The baseline comparison can be best understood by checking Figure. 6, which reports the restoration scores under different video bitrates. We can observe that a higher bitrate brings a better restoration quality, where CaDM significantly outperforms other baselines. This comparison explicitly demonstrates CaDM’s superiority in bitrate saving and video restoration.

4.3. Ablation Studies

Effect of Resolution Scaling Factor. We inspect how resolution scaling factor impacts DaCM’s restoration performance. A larger factor will compress more visual information on original frames and make the restoration procedure harder, thus leading to a worse FID score. As shown in Figure. 7, our CaDM significantly outperforms the baselines with much better FID scores under different scaling factors. This verifies that CaDM is qualified to deliver commodity 1080p/720p streaming in low-resolution versions while not incurring quality degradation.

Effect of Color Bit-depth. Recall that color bit-depth also directly impacts the restoration performance. We compare CaDM with the baselines by using different bit-depths, ranging from 4 to 8. A lower bit-depth will reduce the color number and lose more distribution information of pixel values, thus also yielding a harder restoration task. Comparison results in Figure. 8 show that our CaDM consistently

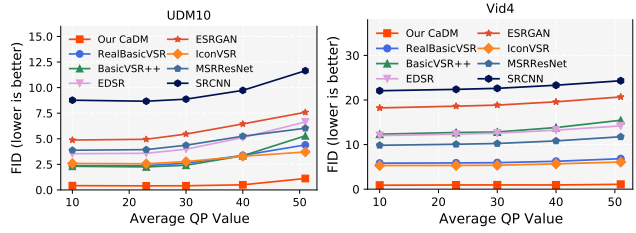


Figure 9. Restoration quality with different QP settings.

achieves the best restoration scores, verifying its powerful synthesis capacity to generate high-fidelity visual details, even in extreme low color space.

Effect of Built-in Bitrate Factors. As an NVS paradigm, CaDM can serve as a general and auxiliary compression-enhancement module to further improve existing video standards, where the settings of their built-in bitrate factors also impact CaDM’s restoration performance. Generally, common video standards (*i.e.*, H.264, H.265 and H.266) conduct spatial-temporal compression through the macroblock-wise bit allocation, which is a kind of data quantization and can be controlled by the *Quantization Parameter* (QP) [53]. In the 24-bit color space (*i.e.*, 8 bit-depth in RGB channels), we unify the QP settings of H.264, H.265 and H.266, ranging from 0 to 51. Given a frame, the lower the average QP is, the more bits will be allocated, thus with the better visual quality. However, a lower QP value will also lead to a larger video bitrate. As shown in Figure. 9, a higher QP will make videos lose more visual information and lead to a worse restoration quality. However, our CaDM consistently outperforms all the baselines with much better FID scores and lower sensitivity to QP degradation. This verifies CaDM is compatible with common video standards.

5. Conclusion

Video streaming is a significant infrastructure to deliver multimedia content and deploy perception services across the Internet. We identify the performance bottleneck on the ingest side and develop new insights into designing efficient NVS frameworks. Aiming at improving the *rate-distortion* trade-off between bitrate saving and quality restoration, we conduct an encoder-decoder synergy and propose the *Codec-aware Diffusion Modeling* (CaDM), a novel NVS paradigm to significantly reduce the streaming delivery bitrates while guaranteeing high restoration quality on the compressed videos. First, CaDM introduces the resolution-color compression to make the encoder fit streamer’s up-link environment. Second, CaDM optimizes the decoder’s enhancement capacity by leveraging the visual-generative property of diffusion models. Evaluations based on public cloud services verify that CaDM effectively achieves an order of magnitude improvement in bitrate saving and holds the state-of-the-art restoration performance in different quality assessment metrics.

References

- [1] Athula Balachandran, Vyas Sekar, Aditya Akella, Srinivasan Seshan, Ion Stoica, and Hui Zhang. Developing a predictive model of quality of experience for internet video. In *Proceedings of the Annual conference of the ACM Special Interest Group on Data Communication on the applications, technologies, architectures, and protocols for computer communication (SIGCOMM)*, pages 339–350. ACM, 2013. 1
- [2] Yochai Blau and Tomer Michaeli. The perception-distortion tradeoff. In *Proceedings of the IEEE Conference on Computer Vision and Pattern Recognition (CVPR)*, pages 6228–6237. Computer Vision Foundation / IEEE Computer Society, 2018. 7
- [3] Kelvin C. K. Chan, Xintao Wang, Ke Yu, Chao Dong, and Chen Change Loy. Basicvsr: The search for essential components in video super-resolution and beyond. In *Proceedings of the IEEE Conference on Computer Vision and Pattern Recognition (CVPR)*, pages 4947–4956. Computer Vision Foundation / IEEE, 2021. 3, 6, 7
- [4] Kelvin C. K. Chan, Shangchen Zhou, Xiangyu Xu, and Chen Change Loy. Basicvsr++: Improving video super-resolution with enhanced propagation and alignment. In *Proceedings of the IEEE/CVF Conference on Computer Vision and Pattern Recognition (CVPR)*, pages 5962–5971. IEEE, 2022. 2, 3, 6, 7
- [5] Kelvin C. K. Chan, Shangchen Zhou, Xiangyu Xu, and Chen Change Loy. Investigating tradeoffs in real-world video super-resolution. In *Proceedings of the IEEE/CVF Conference on Computer Vision and Pattern Recognition (CVPR)*, pages 5952–5961. IEEE, 2022. 3, 6, 7
- [6] Jun-Ho Choi, Jun-Hyuk Kim, Manri Cheon, and Jong-Seok Lee. Deep learning-based image super-resolution considering quantitative and perceptual quality. *Neurocomputing*, 398:347–359, 2020. 3
- [7] Jun-Ho Choi, Huan Zhang, Jun-Hyuk Kim, Cho-Jui Hsieh, and Jong-Seok Lee. Evaluating robustness of deep image super-resolution against adversarial attacks. In *Proceedings of the IEEE/CVF International Conference on Computer Vision (ICCV)*, pages 303–311. IEEE, 2019. 7
- [8] Mengyu Chu, You Xie, Jonas Mayer, Laura Leal-Taixé, and Nils Thuerey. Learning temporal coherence via self-supervision for gan-based video generation. *ACM Trans. Graph.*, 39(4):75, 2020. 3
- [9] Pamela C. Cosman, Karen L. Oehler, Eve A. Riskin, and Robert M. Gray. Using vector quantization for image processing. *Proc. IEEE*, 81(9):1326–1341, 1993. 4
- [10] Mallesh Dasari, Kumara Kahatapitiya, Samir R. Das, Aruna Balasubramanian, and Dimitris Samaras. Swift: Adaptive video streaming with layered neural codecs. In *Proceedings of the USENIX Symposium on Networked Systems Design and Implementation (NSDI)*, pages 103–118. USENIX Association, 2022. 1, 2, 3, 4
- [11] Dandan Ding, Zhan Ma, Di Chen, Qingshuang Chen, Zuo Liu, and Fengqing Zhu. Advances in video compression system using deep neural network: A review and case studies. *Proc. IEEE*, 109(9):1494–1520, 2021. 1
- [12] Florin Dobrian, Vyas Sekar, Asad Awan, Ion Stoica, Dilip Antony Joseph, Aditya Ganjam, Jibin Zhan, and Hui Zhang. Understanding the impact of video quality on user engagement. In *Proceedings of the Annual conference of the ACM Special Interest Group on Data Communication on the applications, technologies, architectures, and protocols for computer communication (SIGCOMM)*, pages 362–373. ACM, 2011. 2
- [13] Chao Dong, Chen Change Loy, Kaiming He, and Xiaoou Tang. Image super-resolution using deep convolutional networks. *IEEE Trans. Pattern Anal. Mach. Intell.*, 38(2):295–307, 2016. 6, 7
- [14] Kuntai Du, Ahsan Pervaiz, Xin Yuan, Aakanksha Chowdhery, Qizheng Zhang, Henry Hoffmann, and Junchen Jiang. Server-driven video streaming for deep learning inference. In *Proceedings of the Annual conference of the ACM Special Interest Group on Data Communication on the applications, technologies, architectures, and protocols for computer communication (SIGCOMM)*, pages 557–570. ACM, 2020. 2
- [15] Kuntai Du, Qizheng Zhang, Anton Arapin, Haodong Wang, Zhengxu Xia, and Junchen Jiang. Accmpeg: Optimizing video encoding for accurate video analytics. In *Proceedings of the Machine Learning and Systems (MLSys)*. mlsys.org, 2022. 1, 2, 3
- [16] Robert M. Gray, Tamás Linder, and John T. Gill III. Lagrangian vector quantization with combined entropy and codebook size constraints. *IEEE Trans. Inf. Theory*, 54(5):2220–2242, 2008. 4
- [17] H.264. H.264 official website. <https://www.itu.int/rec/T-REC-H.264>, 2023. 2, 3, 6
- [18] H.265. H.265 official website. <https://www.itu.int/rec/T-REC-H.265>, 2023. 2, 3, 6
- [19] H.266. H.266 official website. <https://www.itu.int/rec/T-REC-H.266>, 2023. 2, 3, 6
- [20] Martin Heusel, Hubert Ramsauer, Thomas Unterthiner, Bernhard Nessler, and Sepp Hochreiter. Gans trained by a two time-scale update rule converge to a local nash equilibrium. In *Proceedings of the Annual Conference on Neural Information Processing Systems (NeurIPS)*, pages 6626–6637, 2017. 7
- [21] Jonathan Ho, Ajay Jain, and Pieter Abbeel. Denoising diffusion probabilistic models. In *Proceedings of the Annual Conference on Neural Information Processing Systems (NeurIPS)*, 2020. 3
- [22] Alain Horé and Djemel Ziou. Image quality metrics: PSNR vs. SSIM. In *Proceedings of the International Conference on Pattern Recognition (ICPR)*, pages 2366–2369. IEEE Computer Society, 2010. 7
- [23] Randell Jesup, Salvatore Loreto, and Michael Tüxen. Webrtc data channel establishment protocol. *RFC*, 8832:1–12, 2021. 1
- [24] Xue Jiang, Xiulian Peng, Chengyu Zheng, Huaying Xue, Yuan Zhang, and Yan Lu. End-to-end neural speech coding for real-time communications. In *Proceedings of the IEEE International Conference on Acoustics, Speech and Signal Processing (ICASSP)*, pages 866–870. IEEE, 2022. 1
- [25] Justin Johnson, Alexandre Alahi, and Li Fei-Fei. Perceptual losses for real-time style transfer and super-resolution. In

- Proceedings of the European Conference on Computer Vision (ECCV)*, volume 9906 of *Lecture Notes in Computer Science*, pages 694–711. Springer, 2016. 1
- [26] Jaehong Kim, Youngmok Jung, Hyunho Yeo, Juncheol Ye, and Dongsu Han. Neural-enhanced live streaming: Improving live video ingest via online learning. In *Proceedings of the Annual conference of the ACM Special Interest Group on Data Communication on the applications, technologies, architectures, and protocols for computer communication (SIGCOMM)*, pages 107–125. ACM, 2020. 1, 2, 3, 4
- [27] Jiwon Kim, Jung Kwon Lee, and Kyoung Mu Lee. Accurate image super-resolution using very deep convolutional networks. In *Proceedings of the IEEE Conference on Computer Vision and Pattern Recognition (CVPR)*, pages 1646–1654. IEEE Computer Society, 2016. 1
- [28] Jonathan Lennox, Kevin Gross, Suhas Nandakumar, Gonzalo Salgueiro, and Bo Burman. A taxonomy of semantics and mechanisms for real-time transport protocol (rtp) sources. *RFC*, 7656:1–46, 2015. 1
- [29] Jiahao Li, Bin Li, and Yan Lu. Deep contextual video compression. In *Proceedings of the Annual Conference on Neural Information Processing Systems (NeurIPS)*, pages 18114–18125, 2021. 1
- [30] Tong Li, Kai Zheng, Ke Xu, Rahul Arvind Jadhav, Tao Xiong, Keith Winstein, and Kun Tan. TACK: improving wireless transport performance by taming acknowledgments. In *Proceedings of the Annual conference of the ACM Special Interest Group on Data Communication on the applications, technologies, architectures, and protocols for computer communication (SIGCOMM)*, pages 15–30. ACM, 2020. 2
- [31] Bee Lim, Sanghyun Son, Heewon Kim, Seungjun Nah, and Kyoung Mu Lee. Enhanced deep residual networks for single image super-resolution. In *Proceedings of the IEEE Conference on Computer Vision and Pattern Recognition (CVPR)*, pages 1132–1140. IEEE Computer Society, 2017. 1, 3, 6, 7
- [32] Ken K. Lin and Robert M. Gray. Vector quantization of video with two codebooks. In *Data Compression Conference (DCC)*, page 537. IEEE Computer Society, 1999. 4
- [33] Ce Liu and Deqing Sun. On bayesian adaptive video super resolution. *IEEE Trans. Pattern Anal. Mach. Intell.*, 36(2):346–360, 2014. 6, 7
- [34] Dong Liu, Yue Li, Jianping Lin, Houqiang Li, and Feng Wu. Deep learning-based video coding: A review and a case study. *ACM Comput. Surv.*, 53(1):11:1–11:35, 2020. 1
- [35] Jing Liu, Pingping Liu, Yuting Su, Peiguang Jing, and Xiaokang Yang. Spatiotemporal symmetric convolutional neural network for video bit-depth enhancement. *IEEE Trans. Multimed.*, 21(9):2397–2406, 2019. 1, 4
- [36] Jiaming Liu, Ming Lu, Kaixin Chen, Xiaoqi Li, Shizun Wang, Zhaoqing Wang, Enhua Wu, Yurong Chen, Chuang Zhang, and Ming Wu. Overfitting the data: Compact neural video delivery via content-aware feature modulation. In *Proceedings of the IEEE/CVF International Conference on Computer Vision (ICCV)*, pages 4611–4620. IEEE, 2021. 1, 2
- [37] Jing Liu, Ziwen Yang, Yuting Su, and Xiaokang Yang. Tanet: Target attention network for video bit-depth enhancement. *IEEE Trans. Multimed.*, 24:4212–4223, 2022. 1, 4
- [38] Tom D. Lookabaugh, Eve A. Riskin, Philip A. Chou, and Robert M. Gray. Variable rate vector quantization for speech, image, and video compression. *IEEE Trans. Commun.*, 41(1):186–199, 1993. 4
- [39] Guo Lu, Wanli Ouyang, Dong Xu, Xiaoyun Zhang, Chunlei Cai, and Zhiyong Gao. DVC: an end-to-end deep video compression framework. In *Proceedings of the IEEE Conference on Computer Vision and Pattern Recognition (CVPR)*, pages 11006–11015. Computer Vision Foundation / IEEE, 2019. 1
- [40] Andreas Lugmayr, Martin Danelljan, Andrés Romero, Fisher Yu, Radu Timofte, and Luc Van Gool. Repaint: Inpainting using denoising diffusion probabilistic models. In *Proceedings of the IEEE/CVF Conference on Computer Vision and Pattern Recognition (CVPR)*, pages 11451–11461. IEEE, 2022. 3, 7
- [41] Di Ma, Fan Zhang, and David R. Bull. Gan-based effective bit depth adaptation for perceptual video compression. In *Proceedings of the IEEE International Conference on Multimedia and Expo (ICME)*, pages 1–6. IEEE, 2020. 1
- [42] Sachit Menon, Alexandru Damian, Shijia Hu, Nikhil Ravi, and Cynthia Rudin. PULSE: self-supervised photo upsampling via latent space exploration of generative models. In *Proceedings of the IEEE/CVF Conference on Computer Vision and Pattern Recognition (CVPR)*, pages 2434–2442. Computer Vision Foundation / IEEE, 2020. 3
- [43] Arvind Narayanan, Xumiao Zhang, Ruiyang Zhu, Ahmad Hassan, Shuwei Jin, Xiao Zhu, Xiaoxuan Zhang, Denis Rybkin, Zhengxuan Yang, Zhuoqing Morley Mao, Feng Qian, and Zhi-Li Zhang. A variegated look at 5g in the wild: performance, power, and qoe implications. In *Proceedings of the Annual conference of the ACM Special Interest Group on Data Communication on the applications, technologies, architectures, and protocols for computer communication (SIGCOMM)*, pages 610–625. ACM, 2021. 1
- [44] Netflix. Netflix official website. <https://www.netflix.com/>, 2023. 1, 3
- [45] Minh Nguyen, Ekrem Çetinkaya, Hermann Hellwagner, and Christian Timmerer. Super-resolution based bitrate adaptation for HTTP adaptive streaming for mobile devices. In *Proceedings of the Mile-High Video Conference (MHV)*, pages 70–76. ACM, 2022. 1, 2, 3
- [46] OpenMMLab. Openmmlab dataset. <https://openmmlab.com/dataset>, 2022. 6
- [47] Mirko Palmer, Malte Appel, Kevin Spiteri, Balakrishnan Chandrasekaran, Anja Feldmann, and Ramesh K. Sitaraman. VOXEL: cross-layer optimization for video streaming with imperfect transmission. In *Proceedings of the International Conference on emerging Networking EXperiments and Technologies (CoNEXT)*, pages 359–374. ACM, 2021. 1
- [48] Yanyuan Qin, Shuai Hao, Krishna R. Pattipati, Feng Qian, Subhabrata Sen, Bing Wang, and Chaoqun Yue. ABR streaming of vbr-encoded videos: characterization, challenges, and solutions. In *Proceedings of the International Conference on emerging Networking EXperiments and Technologies (CoNEXT)*, pages 366–378. ACM, 2018. 1
- [49] Robin Rombach, Andreas Blattmann, Dominik Lorenz, Patrick Esser, and Björn Ommer. High-resolution image

- synthesis with latent diffusion models. In *Proceedings of the IEEE/CVF Conference on Computer Vision and Pattern Recognition (CVPR)*, pages 10674–10685. IEEE, 2022. 3, 6, 7
- [50] Chitwan Saharia, Jonathan Ho, William Chan, Tim Salimans, David J. Fleet, and Mohammad Norouzi. Image super-resolution via iterative refinement. *arXiv preprint*, abs/2104.07636, 2021. 3, 5, 7
- [51] Tim Salimans, Ian J. Goodfellow, Wojciech Zaremba, Vicki Cheung, Alec Radford, and Xi Chen. Improved techniques for training gans. In *Proceedings of the Annual Conference on Neural Information Processing Systems (NeurIPS)*, pages 2226–2234, 2016. 7
- [52] Henning Schulzrinne, Stephen L. Casner, Ron Frederick, and Van Jacobson. Rtp: A transport protocol for real-time applications. *RFC*, 1889:1–75, 1996. 1
- [53] Heiko Schwarz, Detlev Marpe, and Thomas Wiegand. Overview of the scalable video coding extension of the H.264/AVC standard. *IEEE Trans. Circuits Syst. Video Technol.*, 17(9):1103–1120, 2007. 8
- [54] Kalpathy Sivaraman and G. Kavitha. Real-time streaming protocol (rtsp). *Eurasian Journal of Analytical Chemistry*, 13:705–709, 2019. 1
- [55] Jae Woong Soh, Gu Yong Park, Junho Jo, and Nam Ik Cho. Natural and realistic single image super-resolution with explicit natural manifold discrimination. In *Proceedings of the IEEE Conference on Computer Vision and Pattern Recognition (CVPR)*, pages 8122–8131. Computer Vision Foundation / IEEE, 2019. 3
- [56] Jiaming Song, Chenlin Meng, and Stefano Ermon. Denoising diffusion implicit models. In *Proceedings of the International Conference on Learning Representations (ICLR)*. OpenReview.net, 2021. 3, 7
- [57] Yang Song, Jascha Sohl-Dickstein, Diederik P. Kingma, Abhishek Kumar, Stefano Ermon, and Ben Poole. Score-based generative modeling through stochastic differential equations. In *Proceedings of the International Conference on Learning Representations (ICLR)*. OpenReview.net, 2021. 3, 7
- [58] Bo Wang, Mingwei Xu, Fengyuan Ren, Chao Zhou, and Jianping Wu. Cratus: A lightweight and robust approach for mobile live streaming. *IEEE Trans. Mob. Comput.*, 21(8):2761–2775, 2022. 2
- [59] Xintao Wang, Liangbin Xie, Chao Dong, and Ying Shan. Real-esrgan: Training real-world blind super-resolution with pure synthetic data. In *Proceedings of the IEEE/CVF International Conference on Computer Vision (ICCV)*, pages 1905–1914. IEEE, 2021. 3, 7
- [60] Xintao Wang, Ke Yu, Shixiang Wu, Jinjin Gu, Yihao Liu, Chao Dong, Yu Qiao, and Chen Change Loy. ESRGAN: enhanced super-resolution generative adversarial networks. In *Proceedings of the European Conference on Computer Vision (ECCV)*, volume 11133 of *Lecture Notes in Computer Science*, pages 63–79. Springer, 2018. 6, 7
- [61] Zhou Wang, Alan C. Bovik, Hamid R. Sheikh, and Eero P. Simoncelli. Image quality assessment: from error visibility to structural similarity. *IEEE Trans. Image Process.*, 13(4):600–612, 2004. 7
- [62] Zelong Wang, Zhenxiao Luo, Miao Hu, Di Wu, Youlong Cao, and Yi Qin. Revisiting super-resolution for internet video streaming. In *Proceedings of the 32nd Workshop on Network and Operating Systems Support for Digital Audio and Video (NOSSDAV)*, 2022. 2
- [63] Shichang Xu, Subhabrata Sen, and Z. Morley Mao. CSI: inferring mobile ABR video adaptation behavior under HTTPS and QUIC. In *Proceedings of the European Conference on Computer Systems (EuroSys)*, pages 33:1–33:16. ACM, 2020. 1
- [64] Tianfan Xue, Baian Chen, Jiajun Wu, Donglai Wei, and William T. Freeman. Video enhancement with task-oriented flow. *Int. J. Comput. Vis.*, 127(8):1106–1125, 2019. 6
- [65] Francis Y. Yan, Hudson Ayers, Chenzhi Zhu, Sadjad Fouladi, James Hong, Keyi Zhang, Philip Alexander Levis, and Keith Winstein. Learning in situ: a randomized experiment in video streaming. In *Proceedings of the USENIX Symposium on Networked Systems Design and Implementation (NSDI)*, pages 495–511. USENIX Association, 2020. 1
- [66] Junyan Yang, Yang Jiang, and Shuoyao Wang. Enhancement or super-resolution: Learning-based adaptive video streaming with client-side video processing. *arXiv preprint*, abs/2201.08197, 2022. 3
- [67] Xinlei Yang, Hao Lin, Zhenhua Li, Feng Qian, Xingyao Li, Zhiming He, Xudong Wu, Xianlong Wang, Yunhao Liu, Zhi Liao, Daqiang Hu, and Tianyin Xu. Mobile access bandwidth in practice: measurement, analysis, and implications. In *Proceedings of the Annual conference of the ACM Special Interest Group on Data Communication on the applications, technologies, architectures, and protocols for computer communication (SIGCOMM)*, pages 114–128. ACM, 2022. 1
- [68] Hyunho Yeo, Chan Ju Chong, Youngmok Jung, Juncheol Ye, and Dongsu Han. NEMO: enabling neural-enhanced video streaming on commodity mobile devices. In *Proceedings of the Annual International Conference on Mobile Computing and Networking (MobiCom)*, pages 28:1–28:14. ACM, 2020. 1, 2, 3, 4
- [69] Hyunho Yeo, Youngmok Jung, Jaehong Kim, Jinwoo Shin, and Dongsu Han. Neural adaptive content-aware internet video delivery. In *Proceedings of the USENIX Symposium on Operating Systems Design and Implementation (OSDI)*, pages 645–661. USENIX Association, 2018. 1, 3, 4
- [70] Hyunho Yeo, Hwijoon Lim, Jaehong Kim, Youngmok Jung, Juncheol Ye, and Dongsu Han. Neuroscaler: neural video enhancement at scale. In *Proceedings of the Annual conference of the ACM Special Interest Group on Data Communication on the applications, technologies, architectures, and protocols for computer communication (SIGCOMM)*, pages 795–811. ACM, 2022. 1, 2, 3, 4, 6
- [71] Peng Yi, Zhongyuan Wang, Kui Jiang, Junjun Jiang, and Jiayi Ma. Progressive fusion video super-resolution network via exploiting non-local spatio-temporal correlations. In *Proceedings of the IEEE/CVF International Conference on Computer Vision (ICCV)*, pages 3106–3115. IEEE, 2019. 6, 7
- [72] Xiaoqi Yin, Abhishek Jindal, Vyas Sekar, and Bruno Sinopoli. A control-theoretic approach for dynamic adaptive video

- streaming over HTTP. In *Proceedings of the Annual conference of the ACM Special Interest Group on Data Communication on the applications, technologies, architectures, and protocols for computer communication (SIGCOMM)*, pages 325–338. ACM, 2015. [1](#)
- [73] YouTube. Youtube live streaming official website. <https://www.youtube.com/live>, 2022. [1](#)
- [74] Anlan Zhang, Chendong Wang, Bo Han, and Feng Qian. Efficient volumetric video streaming through super resolution. In *Proceedings of the International Workshop on Mobile Computing Systems and Applications (HotMobile)*, pages 106–111. ACM, 2021. [3](#)
- [75] Anlan Zhang, Chendong Wang, Bo Han, and Feng Qian. Yuzu: Neural-enhanced volumetric video streaming. In *Proceedings of the USENIX Symposium on Networked Systems Design and Implementation (NSDI)*, pages 137–154. USENIX Association, 2022. [1](#), [2](#), [3](#)
- [76] Fan Zhang, Mariana Afonso, and David R. Bull. Vistra2: Video coding using spatial resolution and effective bit depth adaptation. *Signal Process. Image Commun.*, 97:116355, 2021. [1](#)
- [77] Kai Zhang, Martin Danelljan, Yawei Li, Radu Timofte, Jie Liu, Jie Tang, Gangshan Wu, Yu Zhu, Xiangyu He, Wenjie Xu, Chenghua Li, Cong Leng, Jian Cheng, Guangyang Wu, Wenyi Wang, Xiaohong Liu, Hengyuan Zhao, Xiangtao Kong, Jingwen He, Yu Qiao, Chao Dong, Xiaotong Luo, Liang Chen, Jiangtao Zhang, Maitreya Suin, Kuldeep Purohit, A. N. Rajagopalan, Xiaochuan Li, Zhiqiang Lang, Jiangtao Nie, Wei Wei, Lei Zhang, Abdul Muqet, Jiwon Hwang, Subin Yang, Jung Heum Kang, Sung-Ho Bae, Yongwoo Kim, Yanyun Qu, Geun-Woo Jeon, Jun-Ho Choi, Jun-Hyuk Kim, Jong-Seok Lee, Steven Marty, Éric Marty, Dongliang Xiong, Siang Chen, Lin Zha, Jiande Jiang, Xinbo Gao, Wen Lu, Haicheng Wang, Vineeth Bhaskara, Alex Levinshstein, Stavros Tsogkas, Allan D. Jepson, Xiangzhen Kong, Tongtong Zhao, Shanshan Zhao, Hrishikesh P. S, Densen Puthussery, C. V. Jiji, Nan Nan, Shuai Liu, Jie Cai, Zibo Meng, Jiaming Ding, Chiu Man Ho, Xuehui Wang, Qiong Yan, Yuzhi Zhao, Long Chen, Long Sun, Wenhao Wang, Zhenbing Liu, Rushi Lan, Rao Muhammad Umer, and Christian Micheloni. AIM 2020 challenge on efficient super-resolution: Methods and results. In *Proceedings of the European Conference on Computer Vision (ECCV)*, volume 12537 of *Lecture Notes in Computer Science*, pages 5–40. Springer, 2020. [6](#), [7](#)
- [78] Yuanxing Zhang, Yushuo Guan, Kaigui Bian, Yunxin Liu, Hu Tuo, Lingyang Song, and Xiaoming Li. EPASS360: qoe-aware 360-degree video streaming over mobile devices. *IEEE Trans. Mob. Comput.*, 20(7):2338–2353, 2021. [2](#)
- [79] Yulun Zhang, Yapeng Tian, Yu Kong, Bineng Zhong, and Yun Fu. Residual dense network for image super-resolution. In *Proceedings of the IEEE Conference on Computer Vision and Pattern Recognition (CVPR)*, pages 2472–2481. Computer Vision Foundation / IEEE Computer Society, 2018. [1](#)
- [80] Zoom. Zoom meeting official website. <https://zoom.us/>, 2022. [1](#)